Journal of Operation and Automation in Power Engineering
Vol. 5, No. 1, June 2017, Pages: 1-9
http://joape.uma.ac.ir

Power Management in a Utility Connected Micro-Grid with Multiple Renewable Energy Sources

A. Hatefi Einaddin[1, 2], A. Sadeghi Yazdankhah[1,], R. Kazemzadeh[1]*
[1]Renewable Energy Research Center, Faculty of Electrical Engineering, Sahand University of Technology, Tabriz, Iran
[2]*Tabriz Electrical Power Distribution Company, Tabriz, Iran*

Abstract- *As an efficient alternative to fossil fuels, renewable energy sources have attained great attention due to their sustainable, cost-effective, and environmentally friendly characteristic. However, as a deficiency, renewable energy sources have low reliability because of their non-deterministic and stochastic generation pattern. The use of hybrid renewable generation systems along with the storage units can mitigate the reliability problem. Hence, in this paper, a grid connected hybrid micro-grid is presented, which includes wind and photovoltaic resources as the primary power sources and a hydrogen storage system (including fuel cell and electrolyzer) as a backup. A new power management strategy is proposed to perform a proper load sharing among the micro-grid units. Hybrid (distributed/central) control method is applied for the realization of the control objectives such as DC bus voltage regulation, power factor control, synchronous grid connection, and power fluctuation suppression. Distributed controllers have the task of fulfilling local control objectives such as MPPT implementation and storage unit control. On the other hand, the central control unit is mainly responsible for power management in the micro-grid. Performance and effectiveness of the proposed power management strategy for the presented micro-grid are verified using a simulation study.*

Keyword: *Micro-grid, Power management, Wind, Photovoltaic, Fuel cell*

1. INTRODUCTION

The ever-increasing demand for energy, exhaustible nature of fossil fuels, and future progress of humankind are deriving the society toward the development of alternative green energy sources. In recent years, various types of renewable energy sources are utilized to produce green energy, among which wind and photovoltaic (PV) energy systems are well developed and widely used [1, 2]. However, they are highly dependent on the climate change that leads to non-deterministic power generation. Combining different types of renewable energy sources can mitigate the reliability problem [3]. Fuel cells (FC) have a great potential to turn into green power sources of the future because of the characteristics like high efficiency, low environmental emissions, high energy density, and rapid technological progress [4]. Hybrid renewable energy system (HRES) consisting of wind and photovoltaic as primary power sources and FC as a secondary (backup) source ensures high quality and reliable power for costumers [5-9]. In order to have more reliable and efficient HRESs, their structures are considered with various energy storage systems such as battery banks, superconducting magnetic energy storage, super capacitors, and hydrogen storage systems [10-15].In the last two decades, many hybrid systems with wind, PV, and FC units have been proposed in the related literature [13,14, 16-18]. Hirose et al. presented a standalone hybrid wind-solar power generation system by applying dump power control [17], which used battery bank and a diesel generator for providing continuous energy flow to the load. When the battery bank was fully charged and renewable power generation exceeded the demand, dump load was switched on to prevent the battery bank from overcharging, which resulted in improving the battery bank's performance and lifetime. However, using diesel generator increased the environmental emissions due to fossil fuel combustion. Moreover, dump loads caused the waste of some portion of the generated renewable energy. In [13], an overall power management strategy was used for an AC-linked standalone hybrid wind-PV-FC system to manage the power flow among different sources of HRES and storage utilities. Each renewable source used a separate DC/AC converter, which made the configuration economically undesirable. In Ref. [14], power management strategy was applied to the wind/PV/FC system in order for hydrogen production and, in Ref. [16], the control of

Received: 10 Oct. 2014
Revised: 13 Jul. and 9 Sep. 2015
Accepted: 12 Dec. 2015
*Corresponding author:
E-mail: sadeghi@sut.ac.ir (A. Sadeghi Yazdankhah)

FC system mitigated the power fluctuation in hybrid wind/PV/FC system. Both [14] and [16] have only performed the instantaneous power management. In [19], a dynamic power management strategy applied for hybrid renewable energy system with flywheel storage system. Apart from the type of renewable sources, the configuration of HRES had a prominent effect on the number of power electronic converters used in the system and its overall control strategy. In [20], main possible topologies for an isolated and grid connected HRES were discussed. Three main configurations of HRES could be classified as: AC-common bus system [21], DC-common bus system [21], and system with hybrid DC/AC bus [22]. Designing a reliable and efficient HRES depends on different aspects of a system such as type of renewable and storage systems, power management strategy, and system configuration.

This paper presents a comprehensive study on designing, control, and power management of a grid connected hybrid (wind/PV/FC) generation system considering all the key aspects of HRES design. Wind and PV are chosen as the primary sources, because in long term consideration, wind and photovoltaic systems have supplementary power profiles [23]. Common DC bus topology along with a central inverter is used for grid connection. Hybrid control of HRES (local and central) is applied to the system. Grid connected inverter is controlled using vector control scheme [24], which enables the system to have a rapid and flexible control on the active and reactive power generated by HRES. Finally, a novel power management strategy is proposed for handling the power flow through different components of HRES. The proper performance and effectiveness of the proposed HRES and control strategy are verified by conducting various simulations in MATLAB/SIMULINK.

2. HRES CONFIGURATION AND UNIT MODELING

2.1. HRES configuration

Figure 1 shows the configuration of the proposed hybrid wind, PV, and FC system. All three sources are connected in parallel to a regulated common DC bus by means of three individual DC-DC boost converters [25]. The topology of regulated common DC bus makes it feasible to integrate different types of energy sources without any synchronization. The system is interfaced to the utility grid through a voltage source inverter (VSI) and controlled by sinusoidal pulse width modulation (SPWM). Two DC-DC converters related to the wind and PV systems are responsible for adjusting the operating point of subsystems to get maximum available power. On the other hand, the grid connected inverter is responsible for DC bus voltage regulation and independent control of active and reactive power generations of HRES.

2.2. Unit modeling

The structure of a wind energy conversion system (WECS) is illustrated in Fig. 1. The wind turbine absorbs wind energy, and permanent magnet synchronous generator (PMSG) converts it into electrical AC power. Compared with the other types of generators, PMSG is highly preferred over wind conversion system because of having higher reliability and efficiency [26]. Below, a three-phase diode rectifier converts the AC power into DC and feeds it to the subsequent DC-DC boost converter, which is responsible for tracking maximum power point (MPP). The mechanical power captured by wind turbine is given by [16]:

$$P_{wind} = \frac{1}{2}\rho A V^3 . C_p(\lambda, \beta) \quad (1)$$

Where, ρ is air density (kg/m), A is the rotor's swept area (m^2), and V is wind speed (m/s). C_p is the energy conversion efficiency of wind turbine which is the function of pitch angle of turbine blades (β) and tip speed ratio (λ_{tip}). The value of tip speed ratio can be calculated by [16]:

$$TSR = \lambda_{tip} = \frac{r.\omega}{V_{wind}} \quad (2)$$

Where, r *and* ω are the radius and rotational speed (rad/sec) of wind turbine blades, respectively. Every wind turbine has a unique optimal tip speed ratio λ_{opt}, which makes the value of C_p maximum. In this paper, perturb and observation method (P&O) [27] is implemented for the DC-DC converter. This method is an iterative solution to find MPP. The algorithm perturbs the operating point of the system (for example, by increasing or decreasing the duty cycle of DC-DC converters) and, then, observes the direction of output power changes. If output power is increased, the perturbation is resumed in the same direction; otherwise, the direction of perturbation will change to impel the system's operating point toward MPP.

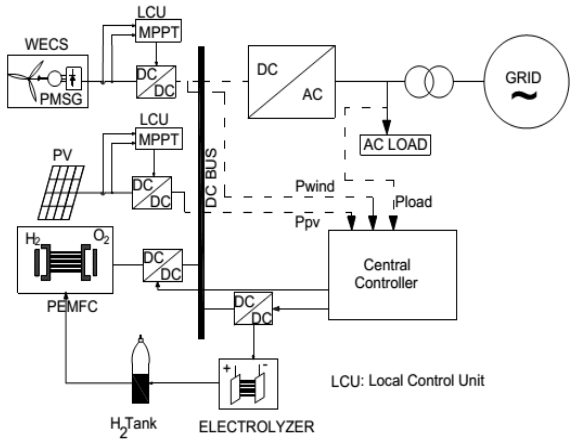

Fig. 1. Block diagram of HRES configuration.

2.2.1 Photovoltaic system

Photovoltaic cells are made of semiconductor materials and convert sunlight directly into electrical energy. The V-I characteristic equation for a PV cell with single diode model can be written as [28]:

$$I = I_{PH} - I_s\left[\exp\left(\frac{q}{kT_c\rho}(V + RI)\right) - 1\right] - \frac{V + R_s I}{R_p} \quad (3)$$

where I_{PH} is the photo current which is mainly the function of solar radiation and cell temperature [29]. T_C is the cell's operating temperature in Kelvin *(K)*, which is calculated from the cell's thermal model [29]. I_S is the diode saturation current, k stands for Boltzmann's constant, ρ is an ideality factor of the diode q representing the single electron charge ($1.6\times10^{-19}{}^{o}C$), and R_p and R_S describe the parallel and series resistances in PV cell model. The process of generating electrical energy from solar radiation has low efficiency; therefore, it should be guaranteed that the maximum available power is captured by the photovoltaic system, which is done by adjusting the operating point of system through the MPPT controller as the climate or load change occurs. In this paper, the direct incremental conductance (IC) [30, 31] method is used for MPPT implementation.

2.2.2 Fuel cell

Fuel cell is a static device that directly converts chemical energy into electrical energy. Compared with internal combustion generators, the efficiency of FC is high (up to 65 percent), which s because of direct energy conversion and presence of no moving parts [32]. Although there are many types of FCs, proton exchange membrane (PEM) fuel cell is the most promising type for hybrid generation system applications because of advantages such as high efficiency, high energy density, relatively long life, adjustability to changes in power demand, low working temperature (80-100ºC), and fast start up [10, 33-35].

For a PEMFC with N series cells, the output voltage can be written as:

$$V_{FC} = N_{cell}V_{cell} = N_{cell}\left[E - V_{act} - V_{ohm} - V_{mass}\right] \quad (4)$$

E is the open circuit voltage of fuel cell described by Nernst equation [34]. V_{act} is the activation loss related to the energy required by the catalyst to commence the chemical reaction [34]. The ohmic loss (V_{ohm}), is the voltage drop related to the resistance of electrodes and electrolyte. V_{mass} is the voltage drop due to the difficulty in mass transportation at high currents. The mathematic description of activation, ohmic, and transmission loss can be stated as [34]:

$$V_{act} = \eta + a.(T - 298) + T.b.\ln(I) \quad (5)$$

$$V_{ohm} = R_{ohm}\times I = (R_0 + K_{RI}I - K_{RT}T)\times I \quad (6)$$

$$V_{mass} = -\frac{RT}{2F}.\ln\left(1 - \frac{1}{I_{\text{limit}}}\right) \quad (7)$$

Where R_0, K_{RI}, K_{RT}, η, a, and b are empirical constants. I_{limit} is the minimum current of FC. As can be obvious from the aforementioned equations, value of cell temperature is needed for FC modeling, which should be extracted from the thermal model of the fuel cell. In this paper, thermal modeling of FC is considered based on the model proposed in [34].

2.2.3 Electrolyzer

FC stack needs pure hydrogen as a fuel to generate electric power. Hydrogen cannot be found freely at nature and should be generated by molecular decomposing which is an energy consuming process. An electrolyzer is a popular device to decompose water to its constituting elements (hydrogen and oxygen) by passing direct current through water [21]. The rate of hydrogen generation depends on the electrolyzer current; so, an electrolyzer can be considered a voltage-sensitive variable DC load. In this paper, electrolyzer is simulated based on the model developed in [13].

3. POWER MANAGEMENT OF HRES

In order to design system controllers, it is essential to comprehend the HRES operation mechanism. The main goal of this system is to provide renewable energy to the locally connected AC loads while suppressing inherent power fluctuations of renewable sources. Although the average value of load demand is usually known, the instantaneous variation of demand and stochastic nature of renewable power make it impossible to have balanced generation and consumption. It may be assumed that the utility grid connected to the HRES can compensate for the power mismatch between renewable sources and load demand. This issue is true in theory; but, from the technical and economic points of view, it is an undesirable and somewhat unfeasible solution as explained below. The peak value of local load occurs at the peak time of the grid, at which the cost of energy is usually more expensive than the normal loading hours. On the other hand, the lowest demand of the local load occurs when the load demand is also low in the utility grid. Hence, the utility grid does not admit the excess power. Therefore, the surplus energy would be directed to the dump load to prevent the system from overloading. Wasting the surplus power at dump load is not an efficient solution; hence, in this paper, hydrogen-based storage system (FC and electrolyzer) is used to overcome power fluctuation problem in HRES. A power management strategy is proposed to control the charging and discharging process of hydrogen storage system, and control the power exchange between the system and main grid by

considering the system net power. The proposed power management strategy is depicted in Fig. 2 and system net power is calculated as follows:

$$P_{net} = P_{PV} + P_{wind} - P_{Load} \quad (8)$$

When the sum of generated power from renewable sources is higher than the load demand, the value of P_{net} is positive and system works in excess power mode (EPM). In this mode, the preference is given to store the excess power as hydrogen, which is done by an electrolyzer. The algorithm checks the current charge level of hydrogen; if the hydrogen storage is not fully charged, the electrolyzer will be switched on to consume excess power for hydrogen generation. The electrolyzer stays on until reaching the full charge level or changing the sign of P_{net}. At the second priority, whenever the excess power is not admitted by the storage system (state of full charge), power is injected into the main grid by the grid connected central inverter. In contrast to EPM, when P_{net} is negative, the system goes to shortage power mode (SPM). In this mode, FC is first switched on to compensate for power shortage and stays on until the volume of hydrogen reaches below the permitted minimum level or the sign of P_{net} is changed. At the second priority, whenever the FC cannot provide the unmet power, local load will be fed from the main grid. In brief, the proposed algorithm continually controls the power balance status in HRES and, then, determines the reference power for backup systems, i.e. fuel cell, electrolyzer, and utility grid.

4. CONTROL OF HRES

In a micro-grid with various types of energy and storage systems, each component should be controlled to enhance the system's operational goals. In this paper, this issue is done by employing local control scheme for each component. For renewable sources (wind and PV), the aim of local controller is to track MPP in any condition. For the storage system, local controller provides the reference power extracted from upstream controllers. Ata higher level, all the HRES units (sources and converters) have interacted relations with each other. Therefore, the supervisory or central control unit should acquire data from different parts of the system and make proper decision to maintain the stable operation of HRES. Actually, the main task of central controller is to continuously perform the proposed power management strategy (Fig. 2) based on the data coming from the measurement devices. Fig. 1 shows the schematic block diagram of the proposed local and central control system.

4.1 Control of grid side converter

Grid side converter is a VSI with sinusoidal pulse width modulation switching scheme, which controls the magnitude and frequency of the output voltage. In addition, in this paper, DC bus voltage regulation and power factor control of the HRES are executed by controlling grid side converter through a vector control scheme, which is a desirable method because of its fast dynamic response and ability of efficient decoupled control of active and reactive power [24]. The schematic block diagram of this method is shown in Fig. 3. According to this figure, instantaneous power equation in abc stationary frame is [36]:

$$P(t) = \begin{bmatrix} V_a & V_b & V_c \end{bmatrix} \begin{bmatrix} i_a & i_b & i_c \end{bmatrix}^t \quad (9)$$

Where i_{abc} and V_{abc} are the output currents and voltages of the inverter, respectively. Considering the voltage drop over the inductors of the passive filter (L_f), V_{abc} can be written as:

$$\begin{bmatrix} V_a \\ V_b \\ V_c \end{bmatrix} = R_f \begin{bmatrix} i_a \\ i_b \\ i_c \end{bmatrix} + L_f \frac{d}{dt} \begin{bmatrix} i_a \\ i_b \\ i_c \end{bmatrix} + \begin{bmatrix} V_{a1} \\ V_{b2} \\ V_{c3} \end{bmatrix} \quad (10)$$

Where L_f and R_f are the inductors and resistors of the three phase passive filters, respectively. Also V_{a1}, V_{b1}, and V_{c1} are the inverter output voltages before passive filter.

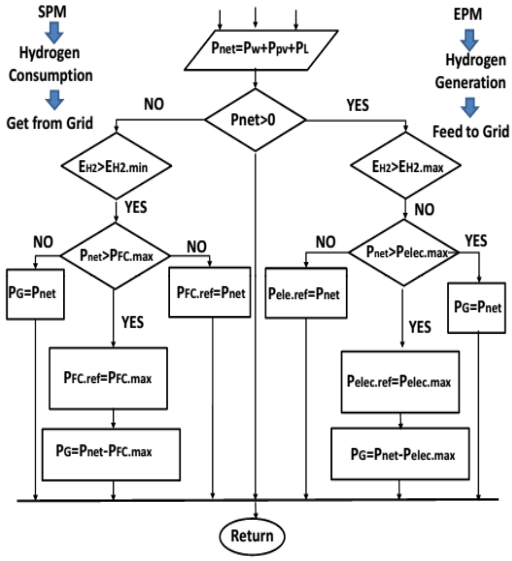

Fig. 2. Flowchart of the proposed power management strategy.

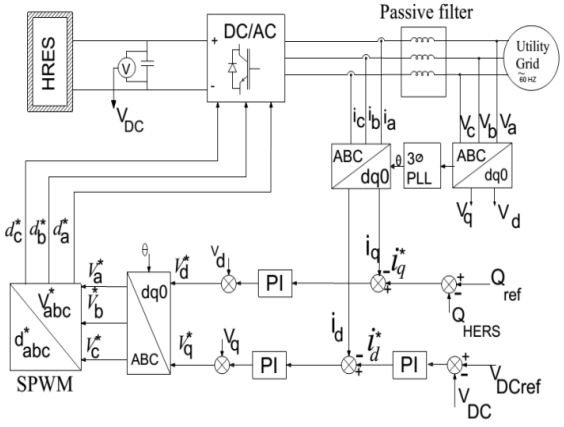

Fig. 3. Vector control scheme applied to the grid side converter.

By employing the park transformation, the equations of instantaneous powers in d-q frame are as follows:

$$P = \frac{3}{2}\left(V_d i_d + V_q i_q\right) \quad (11)$$

$$Q = \frac{3}{2}\left(V_d i_q + V_q i_d\right) \quad (12)$$

For a balanced three phase signal in abc frame, the value of V_q at d-q frame will be equal to zero [36]. Therefore, the active and reactive power equations are simplified as:

$$P = \frac{3}{2}|V|\, i_d \quad (13)$$

$$Q = \frac{3}{2}|V| i_q \quad (14)$$

where $|V|$ is the magnitude of the inverter output voltage. Utilizing the inverter output currents in d-q frame makes it possible to control the active and reactive power independently. The d-axis current is chosen to regulate the DC bus voltage and q-axis current controls the reactive power. In this paper, the unity power factor is considered for HRES control, since the value of i_q is set to zero. The phase angle θ is calculated from the three phase grid voltages by a phase-locked loop (PLL).

5. SIMULATION RESULTS

The SUNPOWER305 solar panel is used as the case study in this paper. The simulated P-V characteristic curve of the SUNPOWER305 module is shown in Fig. 4.

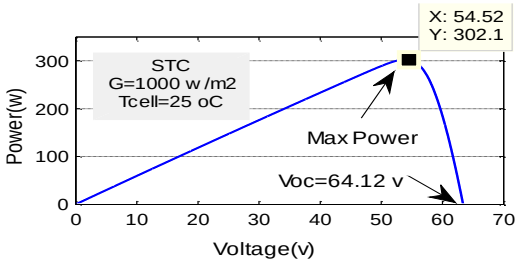

Fig. 4. The p-v characteristic curve of SUNPOWER305.

Figure 5 shows the P-TSR curves of the WECS. Obviously, the value of optimal TSR is independent from wind speed. Fig. 6 depicts the variation of C_p in terms of the rotor speed changes for different wind speeds.

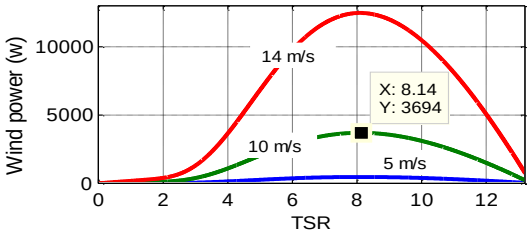

Fig. 5. Power-TSR curves of the simulated wind turbine.

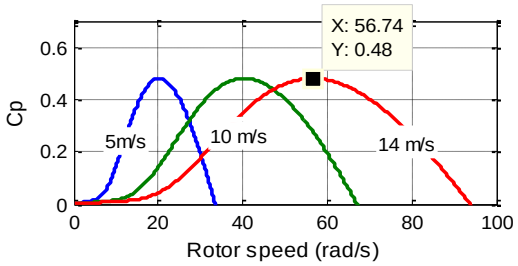

Fig. 6. C_p-rotor speed curves of the wind turbine.

The V-I and P-I characteristic curves of the modeled PEMFC are shown in Figs.7 and 8, respectively. The V-I curve of the simulated electrolyzer is shown in Fig. 9. Following the model validation of HRES components, the overall system performance is studied by conducting two different simulation scenarios. In the first scenario, the behavior of the system for a short period of time (several seconds) is observed. The main goal of this scenario is to evaluate the system performance in fulfilling different control tasks such as DC bus voltage regulation, HRES power factor control, and MPPT control. In addition, the capability of backup units (hydrogen storage system and public grid) for suppressing renewable power fluctuations is studied by directing two separate simulations. In state one, it is assumed that only the public grid should suppress all power fluctuations. Instate two, it is considered that only the storage system is responsible for mitigating power mismatch problem. This situation verifies the effectivness of the peoposed hydrogen storage system forsupressing the renewable power fluctuations. The second senario will study the system'sperformance under variable loads for a 24-h period.

Scenario 1: state one

The hybrid energy system is supposed to provide fixed 9 KW power for the connected AC load at unity power factor despite wind and solar variations. PV array consists of 25 solar panels (5 strings in parallel, each including 5 panels in series, 5x5) with the nominal capacity of 7625 KW. WECS includes one wind turbine with the power curve presented in Fig. 5. The stochastic insulation and wind speed profile, which are applied to the HRES are presented in Fig. 9.

The output power of the PV and WECS isdepictedinFigs.11 and 12, respectively. Total power from renewable sources and constant 9 KW load are illustrated in Fig. 13. It can be observed that the value of net power is more than the load demand in some intervals and less than that in others. Whenever the renewable power exceeds 9 KW, the extra power is fed to the public grid; therefore, the value of P_{grid} is positive. Conversely, when there is power shortage in the system, power from grid is fed to the HRES to meet the 9 KW load; hence, the value of P_{grid} is negative (the second curve in Fig.13).

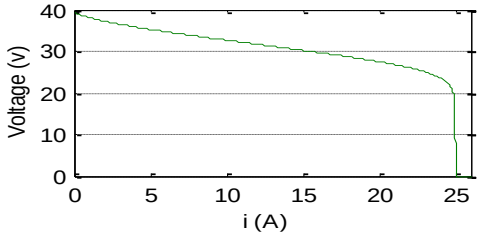

Fig. 7. Fuel cell V-I curve.

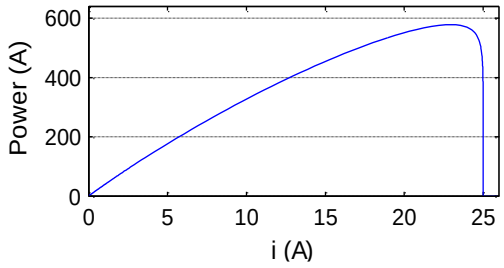

Fig. 8. Fuel cell P-V curve.

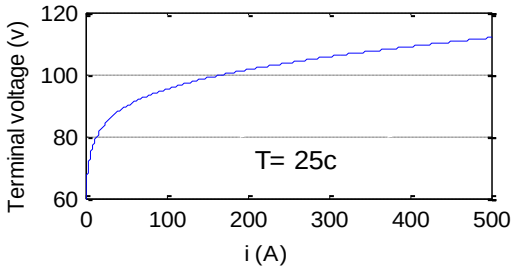

Fig. 9. Electrolyzer V-I curve.

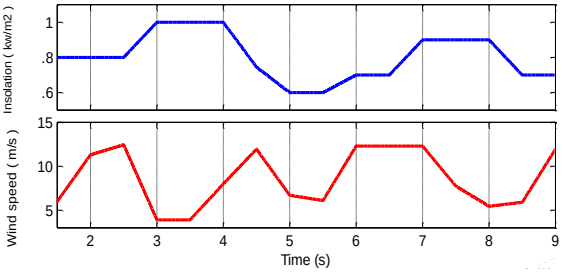

Fig. 10. Insulation and wind speed profile versus time.

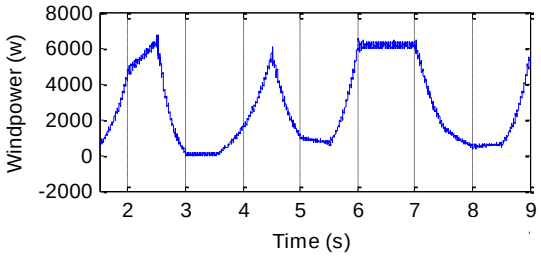

Fig. 11. Generated power by WECS.

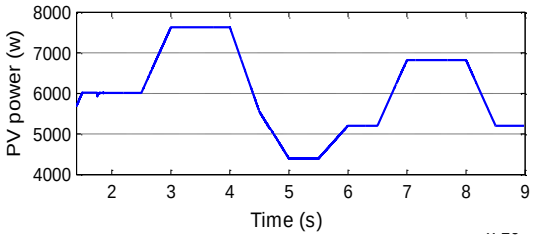

Fig. 12. Generated power by PV system.

Figure 14 shows the profile of active power fed to the load during the simulation period. The result reveals that the applied control is able to suppress renewable power fluctuations and provide fixed power to the load. Another objective of the control system is to regulate DC bus voltage at 500 volt. Fig. 15 shows the profile of DC bus voltage during the system operation, which is fixed around the referenced value with the voltage ripple of less than 0.5 volt. Therefore, it can be concluded that the vector control applied to the grid side converter and the d axis current control of the inverter in d-q frame efficiently make the voltage balance at DC bus by controlling the HRES active power flow.

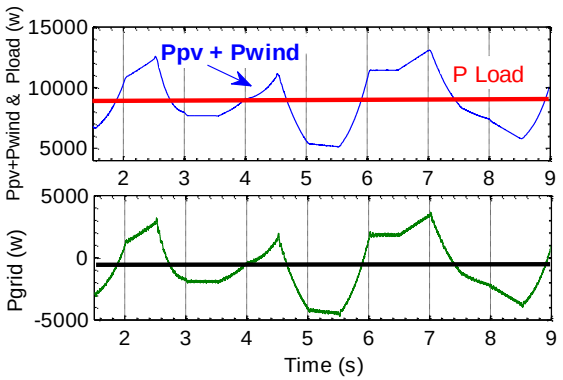

Fig. 13. Active power exchange between HRES and public grid.

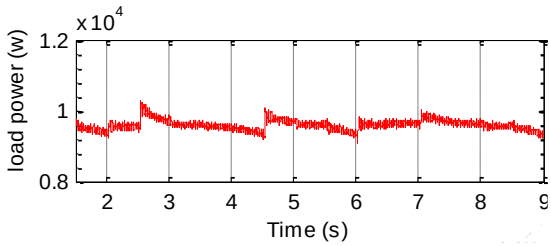

Fig.14. Power fed to the load during simulation period.

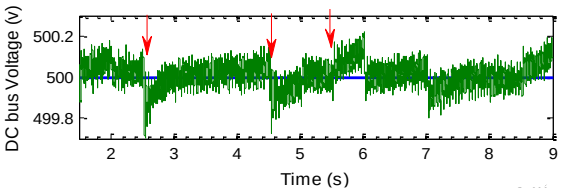

Fig. 15. Profile of DC bus voltage during simulation period.

The last objective of the control scheme is to maintain the active power at unity power factor by setting the value of q axis current (i_q) equal to zero according to (18). The value of measured i_q of the inverter is illustrated in Fig. 16. As expected, i_q follows its reference value and remains at zero in the simulation period. Therefore, the value of reactive power of the inverter is equal to zero, which is shown by plotting the output power of the grid side converter in Fig. 17.

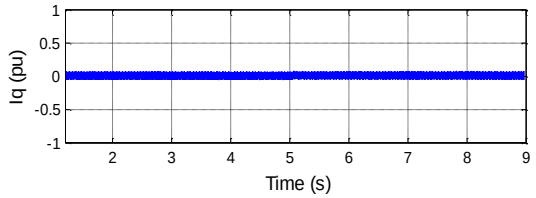

Fig. 16. Value of iq during the simulation period.

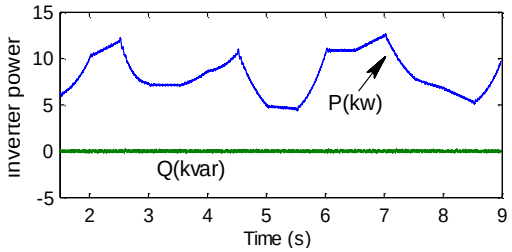

Fig. 17. Active and reactive powers of inverter.

Scenario 1: state two

In this state, it is supposed that the storage system only handles the excess and shortage power problem in HRES. The accomplishment of the control objectives isproved in the pervious section; therefore, they are not repeated in this section. Fig.18 shows the performance of the hydrogen storage system for the same insulation and wind speed profile. When the net power of HRES becomes positive, the electrolyzer starts to consum excess power by producing hydrogen and storing it in thehydrogen tank. Conversely, when the net power becomes negative, FC stack begins to compensate for the short power by consuming hydrogen.

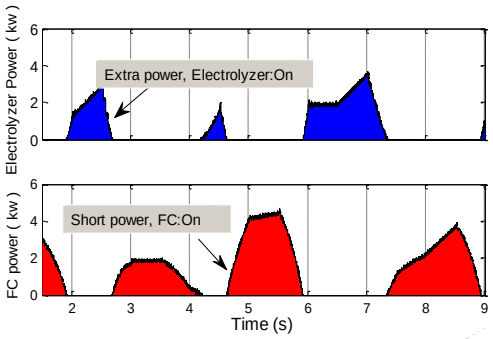

Fig.18. Generated and consumed power by FC and electrolyzer.

Scenario 2:

The second scenario corresponds to the performance of the proposed power management strategy for controlling the power flow between the different components of HRES. In this scenario, relatively long-term simulation is conducted, in which a stochastic load profile with the daily average of 11 kW and peak value of 19 kW is considered. An straightforward method for determining the size of renewable energy sources is to consider the energy balance between the demand and generated renewable energy for certain intervals [13]. It is assumed that the annual capacity factor of the installed wind and photovoltaic energy systems is 0.25; then, the size of renewable sources is determined by the use of energy balance method considering the annual capacity factor. Therefore, a wind energy system with the nominal capacity of 25 kW (for the rated 12 m/s wind speed) and a PV array with 15 kW rated power (for STC condition) is considered. The nominal capacity of FC stack is 20 kW; so, it can provide the peak load, even when there is no generation from renewable sources. The literature review shows that, in an HRES, the amount of excess power is usually less than the half of total renewable power [37]; hence, an electrolyzer with the capacity of 20 kW is chosen. Fig. 19 shows the wind speed insulation (G) and load profile over one day period. The output power of renewable units for the given wind speed and radiation profile is shown in Fig. 20.

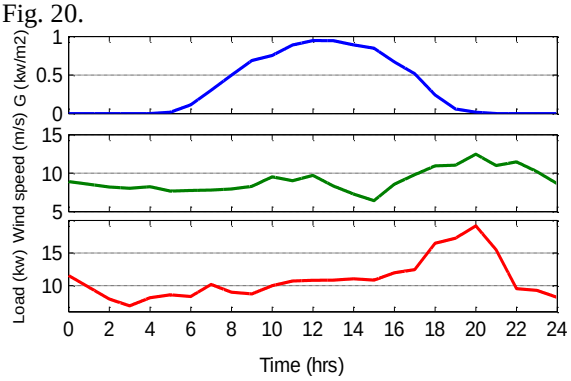

Fig.19. Profile of the applied insulation, wind speed and load.

In order to survey the performance of the central controller, the main outputs of HRES are illustrated in Fig. 21. At the beginning of the simulation, the value of P_{net} is negative which means that the system is in SPM mode. Also, the volume of stored hydrogen energy is half of its maximum value (40 kwh). Therefore, FC stack is on and compensates for the shortage power until the hydrogen level reaches its minimum value. At this point, FC is switched off and public grid is responsible for compensating for the short age power, which is shown in the figure by negative value. Around $t = 7.5\ hrs$, total renewable power exceeds the load power and the system goes to EPM. The primary preference is to convert the excess energy into hydrogen fuel by switching on the electrolyzer system and store it in the hydrogen tank. Around $t = 15\ hrs$, hydrogen level reaches its maximum value and ,from this point on, the excess power will be fed to the grid to protect the system from overloading. It should be noted that, if the value of excess power becomes more than the electrolyzer's nominal power, the electrolyzer will be fixed at its maximum power and the remaining power will fed to the grid. The obtained results revel that the proposed power management strategy effectively chases the load and generation fluctuations and also properly handles the power mismatches in HRES, both in SPM and EPM.

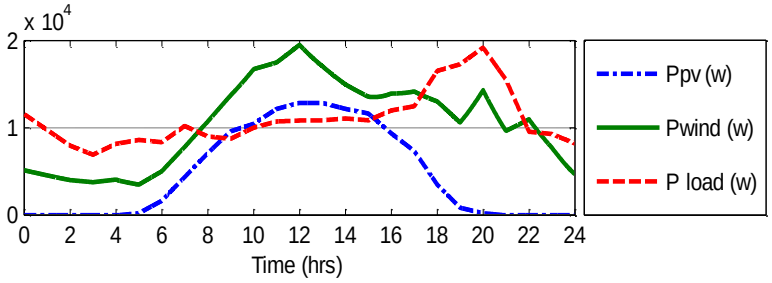

Fig. 20. PV and WECS generated power

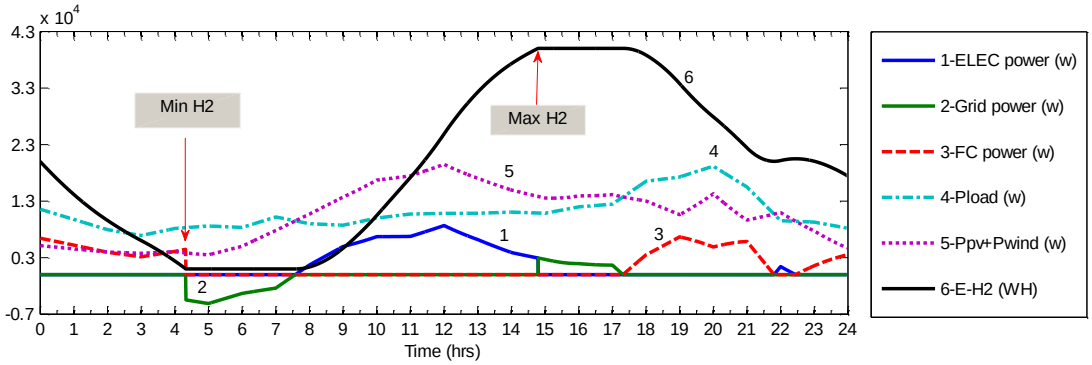

Fig.21. Performance of the proposed power management strategy in HRES control.

6. CONCLUSIONS

In order to survey the performance of the central controller, the main outputs of HRES are illustrated in Fig. 21. At the beginning of the simulation, the value of P_{net} is negative which means that the system is in SPM mode. Also, the volume of stored hydrogen energy is half of its maximum value (40 kwh). Therefore, FC stack is on and compensates for the shortage power until the hydrogen level reaches its minimum value. At this point, FC is switched off and public grid is responsible for compensating for the short age power, which is shown in the figure by negative value. Around $t = 7.5\ hrs$, total renewable power exceeds the load power and the system goes to EPM. The primary preference is to convert the excess energy into hydrogen fuel by switching on the electrolyzer system and store it in the hydrogen tank. Around $t = 15\ hrs$, hydrogen level reaches its maximum value and, from this point on, the excess power will be fed to the grid to protect the system from overloading. It should be noted that, if the value of excess power becomes more than the electrolyzer's nominal power, the electrolyzer will be fixed at its maximum power and the remaining power will fed to the grid. The obtained results revel that the proposed power management strategy effectively chases the load and generation fluctuations and also properly handles the power mismatches in HRES, both in SPM and EPM.

REFERENCES

[1] K. Afshar, A. Shokri Gazafroudi, "Application of stochastic programming to determine operating reserves with considering wind and load uncertainties," *J. Oper. Autom. Power Eng.*, vol. 1, no. 2, pp. 96-109, 2013.

[2] Trends in photovoltaic applications: survey report of selected IEA countries between 1992 and 2004, *Int. Energy Agency Photovoltaics Power Syst. programme*, 2005.

[3] M. Mikati, M. Santos, and C. Armenta, "Electric grid dependence on the configuration of a small-scale wind and solar power hybrid system," *Renewable Energy*, vol. 57, pp. 587-593, 2013.

[4] Z. Tao, B. Francois, M. el Hadi Lebbal, S. Lecoeuche, "Real-Time emulation of a hydrogen-production process for assessment of an active wind-energy conversion system," *IEEE Trans. Ind. Electron.*, vol. 56, no. 3, pp. 737-746, 2009.

[5] T. F. El-Shatter, M. N. Eskander, M. T. El-Hagry, "Energy flow and management system," *Energy Convers. Manage.*, vol. 47, no. 9-10, pp. 1264-1280, 2006.

[6] T. Senjyu, T. Nakaji, K. Uezato, T. Funabashi, "A hybrid power system using alternative energy facilities in isolated island," *IEEE Trans. Energy Convers.*, vol. 20, no. 2, pp. 406-414, 2005.

[7] E. Dursun, O. Kilic, "Comparative evaluation of different power management strategies of a stand-alone PV/Wind/PEMFC hybrid power system," *Int. J. Electri. Power Energy Syst.*, vol. 34, no. 1, pp. 81-89, 2012.

[8] A. Eid, "Utility integration of PV-wind-fuel cell hybrid distributed generation systems under variable

load demands," *Int. J. Electr. Power Energy Syst.*, vol. 62, pp. 689-699, 2014.
[9] M. Taghizadeh, M. Hoseintabar, J. Faiz, "Frequency control of isolated WT/PV/SOFC/UC network with new control strategy for improving SOFC dynamic response," *Int. Trans. Electr. Energy Syst.*, vol. 25, no. 9, pp. 1748-1770, 2015.
[10] M. Uzunoglu, O. C. Onar, M. S. Alam, "Modeling, control and simulation of a PV/FC/UC based hybrid power generation system for stand-alone applications," *Renewable Energy*, vol. 34, no. 3, pp. 509-520, 2009.
[11] P. Thounthong, P. Tricoli, B. Davat, "Performance investigation of linear and nonlinear controls for a fuel cell/supercapacitor hybrid power plant," *Int. J. Electr. Power Energy Syst.*, vol. 54, pp. 454-464, 2014.
[12] S. M. Mousavi, "An autonomous hybrid energy system of wind/ tidal/ microturbine/ battery storage," *Int. J. Electr. Power Energy Syst.*, vol. 43, no. 1, pp. 1144-1154, 2012.
[13] W. Caisheng, M. H. Nehrir, "Power management of a stand-alone wind/photovoltaic/fuel cell energy system," *IEEE Trans. Energy Convers.*, vol. 23, no. 3, pp. 957-967, 2008.
[14] D. Ipsakis, S. Voutetakis, P. Seferlis, F. Stergiopoulos, C. Elmasides, "Power management strategies for a stand-alone power system using renewable energy sources and hydrogen storage," *Int. J. Hydrogen Energy*, vol. 34, no. 16, pp. 7081-7095, 2009.
[15] M. A. Yazdanpanah-Jahromi, S.-M. Barakati, S. Farahat, "An efficient sizing method with suitable energy management strategy for hybrid renewable energy systems," *Int. Trans. Electr. Energy Syst.*, vol. 24, no. 10, pp. 1473-1492, 2014.
[16] N. A. Ahmed, M. Miyatake, A. K. Al-Othman, "Power fluctuations suppression of stand-alone hybrid generation combining solar photovoltaic/wind turbine and fuel cell systems," *Energy Convers. Manage.*, vol. 49, no. 10, pp. 2711-2719, 2008.
[17] T. Hirose, H. Matsuo, "Standalone hybrid wind-solar power generation system applying dump power control without dump load," *IEEE Trans. Ind. Electron.*, vol. 59, no. 2, pp. 988-997, 2012.
[18] S. Saravanan, S. Thangavel, "Instantaneous reference current scheme based power management system for a solar/wind/fuel cell fed hybrid power supply," *Int. J. Electr. Power Energy Syst.*, vol. 55, pp. 155-170, 2014.
[19] G. Boukettaya, L. Krichen, "A dynamic power management strategy of a grid connected hybrid generation system using wind, photovoltaic and Flywheel Energy Storage System in residential applications," *Energy*, vol. 71, pp. 148-159, 2014.
[20] M. S. Carmeli, F. Castelli-Dezza, M. Mauri, G. Marchegiani, D. Rosati, "Control strategies and configurations of hybrid distributed generation systems," *Renewable Energy*, vol. 41, pp. 294-305, 2012.
[21] P. Bajpai, V. Dash, "Hybrid renewable energy systems for power generation in stand-alone applications: A review," *Renewable Sustainable Energy Rev.*, vol. 16, no. 5, pp. 2926-2939, 2012.
[22] L. Xiong, W. Peng, L. Poh Chiang, "A hybrid AC/DC microgrid and its coordination control," *IEEE Trans. Smart Grid*, vol. 2, no. 2, pp. 278-286, 2011.
[23] E. Kabalci, "Design and analysis of a hybrid renewable energy plant with solar and wind power," *Energy Convers. Manage.*, vol. 72, pp. 51-59, 2013.
[24] M. E. Haque, M. Negnevitsky, K. M. Muttaqi, "A novel control strategy for a variable-speed wind turbine with a permanent-magnet synchronous generator," *IEEE Trans. Ind. Appl.*, vol. 46, no. 1, pp. 331-339, 2010.
[25] H. Rashid, *Power Electron.: Circuits, Devices, Appl.*: Pearson Education, 2004.
[26] V. Behjat, A. R. Dehghanzadeh, "Experimental and 3D finite element analysis of a slotless aircored axial flux pmsg for wind turbine application," *J. Oper. Autom. Power Eng.*, vol. 2, no. 2, pp. 121-128, 2014.
[27] M. A. Abdullah, A. H. M. Yatim, C. W. Tan, R. Saidur, "A review of maximum power point tracking algorithms for wind energy systems," *Renewable Sustainable Energy Rev.*, vol. 16, no. 5, pp. 3220-3227, 2012.
[28] H.-L. Tsai, "Insolation-oriented model of photovoltaic module using Matlab/Simulink," *Solar Energy*, vol. 84, no. 7, pp. 1318-1326, 2010.
[29] M. G. Villalva, J. R. Gazoli, E. R. Filho, "Comprehensive approach to modeling and simulation of photovoltaic arrays," *IEEE Trans. Power Electron.*, vol. 24, no. 5, pp. 1198-1208, 2009.
[30] V. Salas, E. Olías, A. Barrado, A. Lázaro, "Review of the maximum power point tracking algorithms for stand-alone photovoltaic systems," *Solar Energy Mater. Solar Cells*, vol. 90, no. 11, pp. 1555-1578, 2006.
[31] C. Hua, J. Lin, H. Tzou, "MPP control of a photovoltaic energy system," *Eur. Trans. Electr. Power*, vol. 13, no. 4, pp. 239-246, 2003.
[32] E. Koutroulis, D. Kolokotsa, A. Potirakis, K. Kalaitzakis, "Methodology for optimal sizing of stand-alone photovoltaic/wind-generator systems using genetic algorithms," *Solar Energy*, vol. 80, no. 9, pp. 1072-1088, 2006.
[33] M. Nayeripour, M. Hoseintabar, T. Niknam, J. Adabi, "Power management, dynamic modeling and control of wind/FC/battery-bank based hybrid power generation system for stand-alone application," *Int. Trans. Electr. Power*, vol. 22, no. 3, pp. 271-293, 2012.
[34] W. Caisheng, M. H. Nehrir, S. R. Shaw, "Dynamic models and model validation for PEM fuel cells using electrical circuits," *IEEE Trans. Energy Convers.*, vol. 20, no. 2, pp. 442-451, 2005.
[35] M. Ansarian, S. M. Sadeghzadeh, M. Fotuhi-Firuzabad, "Optimum generation dispatching of distributed resources in smart grids," *Int. Trans. Electr. Energy Syst.*, vol. 25, no. 7, pp. 1297-1318, 2015.
[36] P. C. Krause, *Anal. electr. mach.*: McGraw-Hill, 1986.
[37] Ø. Ulleberg, "Stand-alone power systems for the future: Optimal design, operation & control of solar-hydrogen energy systems," Norwegian Univ. Sci. Techno, Norway, 1998.